Journal of Magnetic Resonance **156,** 230–241 (2002)
doi:10.1006/jmre.2002.2562

Internuclear Distance Determination of $S = 1$, $I = 1/2$ Spin Pairs Using REAPDOR NMR

Eric Hughes,* Terry Gullion,* Amir Goldbourt,† Shimon Vega,† and Alexander J. Vega‡

*Department of Chemistry, West Virginia University, Morgantown, West Virginia 26506; †Department of Chemical Physics, Weizmann Institute of Science, Rehovot 76100, Israel; and ‡DuPont Central Research and Development, Experimental Station, P.O. Box 80356, Wilmington, Delaware 19880

Received November 14, 2001; revised May 14, 2002; published online July 3, 2002

A universal function is proposed to describe REAPDOR dephasing curves of an observed spin-1/2 nucleus dipole-recoupled to a spin-1 quadrupolar nucleus (^{2}H or ^{14}N). Previous work had shown that, in contrast to REDOR, the shape of the dephasing curve depends on a large number of parameters including the quadrupolar coupling constant and asymmetry parameter, the sample rotation speed, the RF amplitude, and the relative orientations of the quadrupole tensor and the internuclear vector. Here we demonstrate by numerical simulations that the actual dispersion of REAPDOR dephasing curves is quite small, provided the rotation speed and the RF amplitude applied to the quadrupolar nucleus satisfy an adiabaticity condition. The condition is easily met for ^{2}H and is also practically achievable for virtually any ^{14}N-containing compound. This allows the REAPDOR curves to be approximated by a simple universal gaussian-type function, comparison of which with experimental data yields internuclear distances with less than 4% error. The spin dynamics of the recoupling mechanism is discussed. The critical importance of a stable spinning speed for optimizing the signal-to-noise ratio of the ^{13}C echoes is demonstrated and practical suggestions for achieving high stability are presented. Examples of applications of the universal curve are given for ^{2}H/^{13}C and ^{14}N/^{13}C REAPDOR in alanine. © 2002 Elsevier Science (USA)

INTRODUCTION

Measuring dipolar couplings by solid-state NMR has provided important structural information for a wide variety of materials. There are many MAS NMR dipolar recoupling techniques available and most of these have found use in measuring internuclear distances between pairs of spin-1/2 nuclei such as the homonuclear spin pair ^{13}C–^{13}C (*1–17*) and the heteronuclear spin pair ^{13}C–^{15}N (*18–22*). Rotational-echo, double-resonance NMR (REDOR) (*18–20*) is an attractive experiment for measuring heteronuclear dipolar couplings between spin-1/2 nuclei because of its simplicity and ease of data analysis. A particularly useful feature of REDOR is that the dipolar dephasing is characterized by a universal dipolar dephasing curve which depends only on the dipolar interaction for coupled spin-1/2 nuclei.

Only under certain circumstances can REDOR be used in a straightforward manner as a quantitative tool when the heteronuclear spin pair consists of a spin-1/2 nucleus and a quadrupolar nucleus. Fernandez *et al.* demonstrated an ^{27}Al–^{31}P multiple-quantum REDOR (MQ-REDOR) experiment based on observation of the central transition of the ^{27}Al under high-resolution conditions (*23*). The MQ-REDOR experiment works well since the dipolar recoupling pulses are applied to the much easier to manipulate ^{31}P nuclei. At first glance, it might be tempting to perform the REDOR experiment with the observe nucleus being ^{31}P and applying a train of π pulses to the central transition ^{27}Al. This would be beneficial because of the high sensitivity of ^{31}P. Unfortunately, it has been shown that such an experiment is not practical since the REDOR recoupling pulses affect the different transitions of the quadrupolar nucleus with unequal efficiencies. Good progress has been made for the case of ^{13}C-observe REDOR experiments involving ^{2}D (*24–29*). The use of phase-modulated ^{2}D pulses has provided a means to extract ^{13}C–^{2}D dipolar couplings (*26, 27*), and a more recent report shows that the ^{13}C–^{2}D REDOR experiment can be described by a universal dipolar dephasing curve when a ^{2}D composite pulse is used (*29*).

Aside from the special cases mentioned above, it is difficult to determine dipolar couplings between spin-1/2 and quadrupolar nuclei. TRAPDOR (*30–33*), REAPDOR (*34–36*), DEAR (*37*), and RIDER (*38*) are dipolar recoupling experiments designed specifically to recover the dipolar interaction for such spin systems with the observe nucleus being spin-1/2. The DEAR and RIDER experiments take advantage of T_1 relaxation of the quadrupolar nucleus and have the advantages that an RF channel is not necessary for the quadrupolar species and that it is not necessary to know the quadrupolar coupling constant. A disadvantage of DEAR and RIDER is that data analysis requires knowledge of the single-quantum and double-quantum relaxation times. Dipolar recoupling with the TRAPDOR and REAPDOR experiments occurs through the action of an adiabatic-passage pulse applied to the quadrupolar nucleus.

Figure 1 shows the REAPDOR experiment in its simplest form. It consists of an initial $\pi/2$ pulse generating transverse magnetization of the observed $I = 1/2$ nucleus, a train of π pulses applied to I, and a single dipolar recoupling pulse applied to the quadrupolar nucleus S at the midpoint of the pulse sequence. The spacing between adjacent π pulses is $\tau_R/2$, τ_R

1090-7807/02 $35.00
© 2002 Elsevier Science (USA)
All rights reserved.

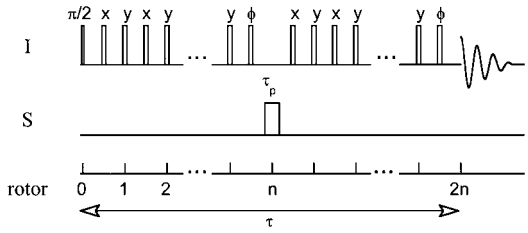

FIG. 1. Pulse sequence for the REAPDOR experiment. The I_x magnetization at $t=0$ may be generated by cross-polarization instead of the $\pi/2$ pulse shown in the figure. The string of pulses in the observe channel are π pulses. The length τ_p of the recoupling pulse is one-third of the rotor period.

being the rotor period, but there is no I pulse located at the midpoint of the dipolar evolution period τ. The single S-spin recoupling pulse serves the same function as the π pulses applied to the nonobserved channel in traditional REDOR experiments in that it changes the z-component of the magnetization of the S spins. REAPDOR is also similar to REDOR in that it is performed as a difference experiment. A control experiment is performed to produce the *full* signal, $S_0(\tau)$, by omitting the S-channel recoupling pulse. The control experiment is used to account for T_2 decay of the I magnetization during the dipolar evolution period. The experiment is repeated to produce the *reduced* signal, $S(\tau)$, by applying the S-spin recoupling pulse. The ratio of the *difference* signal (*full* signal minus the *reduced* signal) to the *full* signal is the REAPDOR fraction $(S_0(\tau)-S(\tau))/S_0(\tau)$.

Unlike REDOR, however, the REAPDOR fraction is not a simple function of the dipolar coupling constant because the S-spin flips are more complex than a simple inversion of their z-component. Ideally, the transitions behave as adiabatic passages, which occur when the time modulated quadrupole splitting crosses through zero during the pulse. But the transitions are not always adiabatic and even when they are, the S-spin RF irradiation induces partial transitions among the magnetic spin states m of the quadrupolar nuclei, rather than affecting a uniform 180° inversion. Consequently, the exact description of the τ dependence of $(S_0-S)/S_0$ depends on many parameters. In principle, data analysis for these experiments requires quantum mechanical calculations which need the quadrupolar coupling constant, the asymmetry parameter of the quadrupolar tensor, the chemical shift anisotropies, the dipolar interaction, the relative orientations between the coupling tensors, the RF field strengths, and the spinning speed as input parameters.

In this paper, we show that the internuclear distance of an $I=1/2$ and $S=1$ spin system can be determined by REAPDOR using a REDOR-like universal dipolar dephasing curve. A simple REAPDOR calculation described by Gullion (*34*) and Ba *et al.* (*39*) already avoided the use of full quantum mechanical calculation by using idealized descriptions of the adiabatic inversions. This approach led to a theoretical universal dipolar dephasing curve that closely matched experimental REAPDOR dephasing curves for $S=1$, $I=1/2$ spin pairs after application of an adjustable multiplication factor. Their results suggested that knowledge of all the aforementioned spin parameters might not be needed in order to obtain quantitative results. We set out to substantiate this concept by performing full quantum mechanical simulations of REAPDOR curves over wide ranges of relevant parameters. The numerical results of this analysis are surveyed in this paper. They allow us to conclude that under broad, experimentally feasible conditions the theoretical REAPDOR curves of $I=1/2$, $S=1$ spin pairs do not deviate substantially from a simple universal function given by

$$(S_0-S)/S_0 = 0.6(1-\exp[-(1.47D\tau)^2]). \qquad [1]$$

The dipolar coupling constant, D, is expressed in Hz and given by

$$D = \gamma_S\gamma_I\hbar/(2\pi r^3), \qquad [2]$$

where r is the internuclear distance. The universal curve is plotted in Fig. 2a. Comparison of experimental data with Eq. [1] gives r with a ±4% accuracy in powder samples provided the following three conditions are met. (a) The values of the

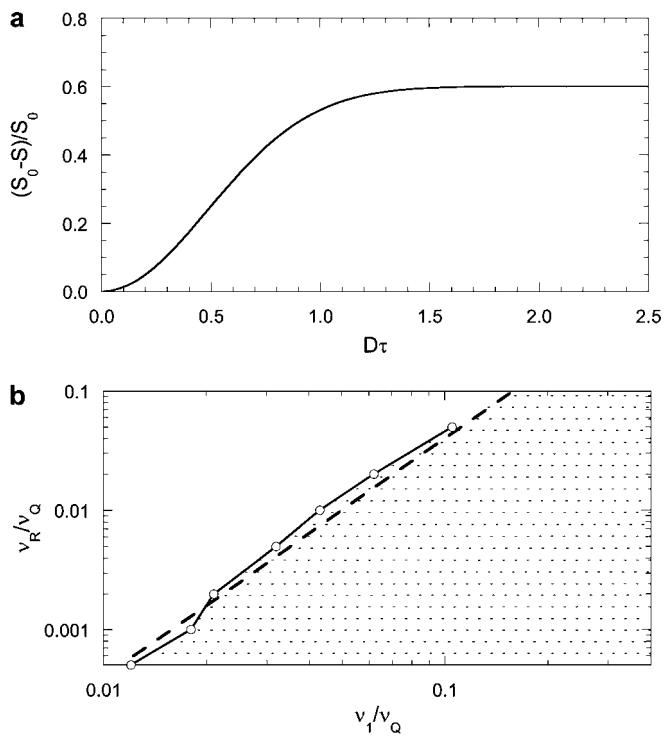

FIG. 2. (a) The universal REAPDOR curve for recoupling of $S=1$ spins given by Eq. [1]. (b) The shaded area indicates the ranges of values of the rotation speed ν_R and the RF amplitude ν_1 for which the universal REAPDOR curve can be used to obtain internuclear distances with ±4% accuracy from experimental REAPDOR fractions. ν_1 and ν_R are normalized to the quadrupole frequency $\nu_Q=(3/2)\chi$. The connected symbols are the boundary points resulting from the numerical analysis presented in this paper. The broken line represents the boundary corresponding to the adiabaticity condition $\nu_1^2/\nu_Q\nu_R > 0.25$.

TABLE 1

Lower Limits of ν_1/ν_Q Ratios for Which the Universal READOR Curve Is Applicable at a Given ν_R/ν_Q Ratio for a ±13% Accuracy of the Dipolar Coupling Constant

ν_R/ν_Q	$(\nu_1/\nu_Q)_{\min}$
0.05	0.105
0.02	0.062
0.01	0.043
0.005	0.032
0.002	0.021
0.001	0.018
0.0005	0.013

recoupling-pulse amplitude ν_1 and the spinning speed ν_R meet the boundary conditions of Table 1, which gives a lower bound for the ratio ν_1/ν_Q for chosen ratios ν_R/ν_Q. The boundary in ν_1/ν_Q, ν_R/ν_Q space is graphically depicted in Fig. 2b. (b) The frequency of the recoupling pulse does not differ from the Larmor frequency of the quadrupolar spins by more than 5% of ν_Q. (c) The duration τ_p of the recoupling pulse is equal to one-third of the rotor cycle. We chose the latter condition as a standard pulse length in accordance with previous work, which showed that $1/(3\nu_R)$ is the optimum pulse duration for obtaining strong dephasing (*39*). In practical applications we envision a simple least-squares curve fitting of the function of Eq. [1] to experimental $(S_0 - S)/S_0$ results, with D as the only adjustable parameter from which the distance r can be determined using Eq. [2]. Corresponding dipolar dephasing curves for $S = 3/2$ and $5/2$ will be presented in a forthcoming publication.

Under Theory we describe how we arrived at the applicability of Eq. [1] using numerical integration of the two-spin density-matrix equation. Calculated dephasing curves for wide ranges of values for the relevant parameters are reviewed and their deviations from the universal curve are evaluated to establish the necessary conditions for successful application of the universal curve. Some aspects of the underlying spin dynamics are also reviewed. Under Experimental, we address specific experimental requirements of the REAPDOR experiments. In particular, we reemphasize that careful synchronization of the pulse sequence with the sample rotation is especially important in the REAPDOR experiment for sensitivity reasons and practical recommendations for achieving stable sample spinning are given. Under Results, experimental REAPDOR data for ^{2}D–^{13}C and ^{14}N–^{13}C spin pairs in alanine are presented and analyzed using the universal curve given in Eq. [1].

THEORY

Spin Interactions

The Liouville–von Neumann equation,

$$(d/dt)\rho(t) = i[\rho(t), H(t)], \qquad [3]$$

governs the evolution of the spin interactions during the REAPDOR experiment (*40*). The density matrix of an I–S two-spin system with $I = 1/2$ and $S = 1$ is $\rho(t)$, and the Hamiltonian, $H(t)$, is (*41, 42*)

$$H(t) = \frac{1}{2}Q(t)\left(S_z^2 - (1/3)S(S+1)\right) + H_Q^{(2)}(t) + \omega_{1S}(t)S_x + \omega_{1I}(t)I_{x,y} + d(t)I_zS_z. \qquad [4]$$

The time dependence of the Hamiltonian originates from the sample spinning at the magic angle and from the pulsed RF fields applied to the I and S spins. The first-order quadrupole splitting, $Q(t)$, is

$$Q(t) = \frac{1}{2}\omega_Q(3\cos^2\theta_Q - 1 - \eta\sin^2\theta_Q\cos 2\phi_Q), \qquad [5]$$

where $\omega_Q = 2\pi\nu_Q$ is the quadrupolar frequency and is related to the quadrupole coupling constant (QCC), $\chi = e^2qQ/h$, by

$$\nu_Q = 3\chi/2S(2S-1) = (3/2)\chi. \qquad [6]$$

The polar angles of the magnetic field with respect to the quadrupole tensor principal axis system are θ_Q and ϕ_Q, and η is the asymmetry parameter of the quadrupole tensor. The time dependence of $Q(t)$ is governed by the sample spinning through its modulation of θ_Q and ϕ_Q and can be written as $Q(t) = \omega_Q g_Q(t)$, where $g_Q(t)$ is an oscillating function of the form (*43*)

$$g_Q(t) = g_1\cos(\omega_R t + \psi_1) + g_2\cos(2\omega_R t + \psi_2). \qquad [7]$$

The parameters g_1, g_2, ψ_1, and ψ_2 are functions of the initial orientation of the crystallites in the rotor frame and of the asymmetry parameter η. The second term in Eq. [4] represents the second order quadrupolar interaction (*41, 42*). In the third term, $\omega_{1S}(t)$ denotes the amplitude profile of the RF pulse applied to the quadrupolar spins. It is determined by the pulse length, τ_p, and the RF amplitude, ν_1. Similarly, $\omega_{1I}(t)$ describes the π pulses applied to the observed spins. The last term in Eq. [4] represents the dipolar interaction. The dipolar splitting, $d(t)$, is given by (*44*)

$$d(t) = \omega_D(1 - 3\cos^2\theta_D), \qquad [8]$$

where $\omega_D = 2\pi D$ is the dipolar coupling constant (see Eq. [2]) and θ_D is the angle between the internuclear vector and the magnetic field. The time dependence of $d(t)$ is governed by the sample spinning and can be written as $d(t) = \omega_D g_D(t)$, where $g_D(t)$ is the periodic function (*43*)

$$g_D(t) = g_1'\cos(\omega_R t + \psi_1') + g_2'\cos(2\omega_R t + \psi_2'). \qquad [9]$$

The parameters of Eq. [9] are functions of the initial polar angles of the internuclear vector with respect to the rotor frame. Not represented in Eq. [4] are terms describing the differences

between the frequencies of the RF pulses and the Larmor frequencies of the S and I spins. Of particular interest would be a term $\Delta\omega S_z$ describing the offset of the recoupling pulse. For example, large offsets lead to ineffective RF irradiation and to reduced REAPDOR fractions. It has been shown that in REAPDOR, as well as in the TRAPDOR experiments, measurements as a function of $\Delta\omega$ can actually be used to estimate the size of ν_Q (*32, 39*). However, in an effort to limit the large number of parameters to be varied in the simulations, we chose to present here only results of simulations where the frequency offset and the chemical shifts of spins I and S were kept equal to zero. Under Results, experimental evidence that the REAPDOR fraction remains unaffected as long as $\Delta\omega$ is less than 5% of ν_Q is presented, in agreement with the findings of Ba *et al.* (*39*).

Numerical Method

The numerical simulations were carried out with a computer program written in a FORTRAN90 programming environment. The program is able to simulate the results of all solid state NMR experiments, involving a spin-half ($I = 1/2$) nucleus coupled to a spin-one ($S = 1$) nucleus. During the calculations of the REAPDOR dephasing curves the initial spin density matrix $\rho(0)$ for each crystallite is set to $I_x + S_z$ and propagated under the MAS Hamiltonian of Eq. [4]. For a polycrystalline sample, a signal $S(\Omega, t) = \mathrm{Tr}(I_-\rho(t))$ is calculated for each crystallite and a powder sum is performed.

The propagation of the density matrix according to Eq. [3] under the time dependent Hamiltonian, $H(t)$, is performed in the following manner: First the time t is divided into time domains starting at t_i and ending at t_{i+1} with $i = 1, 2, \ldots, n$, chosen such that during a single time domain the RF irradiation is either on or off. When RF irradiation is absent during a time domain, $H(t)$ is self-commuting and a propagator can be calculated

$$U(t_i, t_{i+1}) = \exp\left(-i \int_{t_i}^{t_{i+1}} H(t)\, dt\right). \qquad [10]$$

The integral in the exponent is calculated analytically for all first order interactions in Eq. [4]. The second order quadrupolar interaction $H^{(2)}(t)$ is evaluated using the Simpson integration procedure,

$$\int_{t_i}^{t_{i+1}} H^{(2)}(t)\, dt = \sum_{k=0}^{n-1} \frac{\Delta\tau}{6}\Big[H^{(2)}(t_i + k\tau) + 4H^{(2)}\left(t_i + \left(k + \frac{1}{2}\right)\tau\right) + H^{(2)}(t_i + (k+1)\tau)\Big], \qquad [11]$$

where the time domain is divided into small steps $\tau = (t_i - t_{i+1})/n$. In the presence of RF irradiation during a time domain, $H(t)$ is not self-commuting and the Dyson order operator $\hat{T}$ must be used to calculate the propagator. Dividing the time domains with RF irradiation present into small steps $\tau = (t_i - t_{i+1})/n$, $U(t_i, t_{i+1})$ can be evaluated by using

$$U(t_i, t_{i+1}) = \prod_{k=0}^{n-1} \exp\Big\{-iH\left(t_i + \left(k + \frac{1}{2}\right)\tau\right)\tau + \frac{1}{12}[H(t_i + k\tau), H(t_i + (k+1)\tau)]\tau^2\Big\}. \qquad [12]$$

Typical values for the time steps in Eqs. [11] and [12] were 0.5 μs. The final value of $(S_0 - S)/S_0$ was evaluated by the appropriate summation of the expectation value of I_- at $t = \tau$ for 300 powder orientations (*45*).

Numerical Results

The results of numerical simulations are now reviewed in two stages. First we quantitate the REAPDOR uncertainty caused by lack of knowledge of the parameters that define the relative orientations of the quadrupolar and dipolar tensors. These parameters include the quadrupole asymmetry parameter η and the polar angles θ and ϕ of the internuclear vector with respect to the quadrupolar principal axis system. Then we trace the boundaries of a useful range of the experimental parameters ν_1 and ν_R for which the use of a universal READOR dephasing curve is valid. Since only the relative values of ν_1, ν_R, and ν_Q are of relevance, the results are reported in terms of the ratios ν_1/ν_Q and ν_R/ν_Q.

Figure 3 displays two sets of calculated REAPDOR curves. Each set shows the results for all 17 distinct combinations of three η values (0, 0.5, 1), three θ values (0, 45°, 90°), and three ϕ values (0, 45°, 90°). Two sets of constant ν_Q, ν_1, and ν_R parameters were chosen for these calculations (see figure caption). The simulations were done for a constant dipolar parameter, D, and the resulting curves were plotted as a function of $D\tau$. Curve fittings to the universal curve yield apparent dipolar coupling constants D_{fit} that deviate from the actual D value used in the simulation by -8% to $+10\%$ in Fig. 3a (-8% for $\eta = 0, \theta = 90°$; $+10\%$ for $\eta = 0.5, \theta = 90°, \phi = 45°$) and by -13% to $+13\%$ in Fig. 3b (-13% for $\eta = 1$, $\theta = 90°$, $\phi = 45°$; $+13\%$ for $\eta = 0$, $\theta = 0°$). From these and many other (not shown) examples we conclude that, provided ν_1 and ν_R fall in the allowed region indicated in Fig. 2b, a comparison with the universal curve yields a D_{fit} that never deviates more than $\pm 13\%$ from the actual D. Hence, the inherent uncertainty in the internuclear distance r is $\pm 4\%$.

In choosing a simple mathematical form of the universal curve (Eq. [1]) we were guided by two criteria, one being that the average asymptotic value at large $D\tau$ is about 0.6 and the other that the slope and curvature of the curves for $D\tau$ values below ~ 1 should match the average calculated curve. We did not attempt to account for other recurrent features in the simulated curves, such as the maximum around $D\tau = 1.8$. Practical reasons for this simplification were that the exact dephasing behavior at $D\tau > 1$

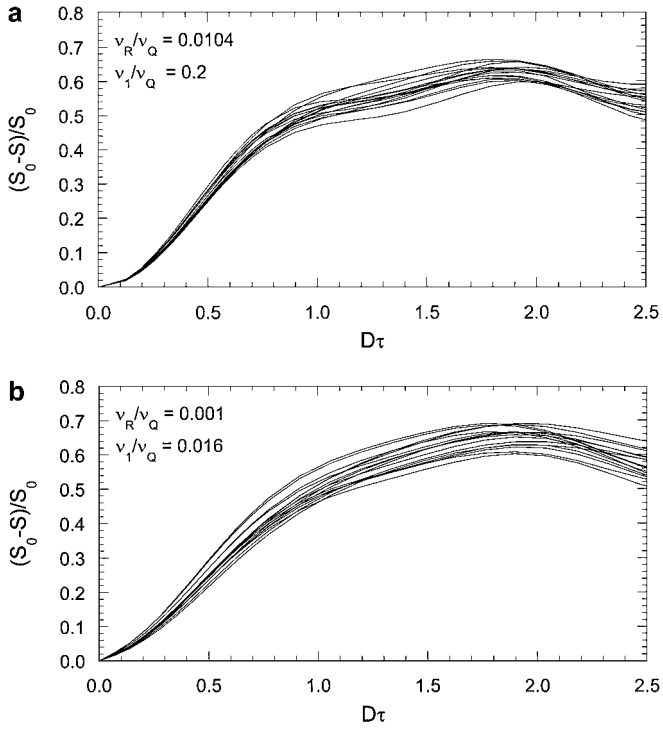

FIG. 3. REAPDOR dephasing curves for recoupling of spin-1 nuclei calculated with the indicated ratios of the rotation speed ν_R, the recoupling pulse amplitude ν_1, and the quadrupole frequency ν_Q. Each graph shows a superposition of the results for 17 combinations of η, θ, and ϕ (see text). Actual parameters used in the calculations: (a) $\nu_Q = 600$ kHz, $\nu_1 = 120$ kHz, $\nu_R = 6.25$ kHz, $D = 200$ Hz. (b) $\nu_Q = 5000$ kHz, $\nu_1 = 80$ kHz, $\nu_R = 5$ kHz, $D = 160$ Hz.

is of minor significance since the τ region of highest sensitivity of $(S_0 - S)/S_0$ to the value of D is below $D\tau = 1$. Furthermore, the shapes of the undulations of the curve above $D\tau = 1$ vary too much from case to case to be able to be captured in a universal mathematical form. This is in contrast to REDOR where the exact shape of the dephasing curve at longer τ values is always the same and, as such, provides the means for deconvolution of multiple interatomic distances (*46*). Nevertheless, theoretical arguments to be presented under Spin Dynamics below help explain the maxima around $D\tau = 1.8$ in REAPDOR curves.

A large set of additional REAPDOR curves was simulated with varying ν_Q, ν_1, and ν_R parameters. Figure 4 shows some examples illustrating the effect of ν_1 variation when the other parameters are kept constant. The quadrupole frequencies in Figs. 4a and 4b are typical for ^2D and ^{14}N, respectively. These figures include calculated curves that agree well with the universal curve and several that deviate significantly from the universal curve. Curve fitting gives D_{fit} values that deviate $\leq$6% from the actual D for the four best fitting curves and $\geq$24% for the three that deviate the most (see figure caption for detailed results).

A more comprehensive summary of the numerical REAPDOR results is shown in Fig. 5 in the form of plots of curve-fitted D_{fit}/D ratios vs ν_1/ν_Q for six ν_R/ν_Q ratios. All curves were calculated for one single set of orientational parameters, i.e., $\eta = 0, \theta = 90°$. The other parameters used in the actual calculations are listed in Table 1. The plots in Fig. 5 served as the basis for the establishment of the boundary of the usable region drawn in Fig. 2b. For each ν_R/ν_Q ratio, the lower limit of ν_1/ν_Q was somewhat arbitrarily determined as 15% above the point in Fig. 5 where D_{fit}/D crosses the 90% level. The criteria presented above could be interpreted such that the lower limit should coincide with the exact point where D_{fit} begins to deviate less than 13% from D. However, we adopted an extra margin to allow for uncertainties arising from the variations in η, θ, and ϕ which were not evaluated explicitly for every point in Fig. 5. The chosen boundary points are indicated with arrows in Fig. 5 and they are also listed in Table 1.

Spin Dynamics

The main objective of this paper was to demonstrate the validity of the universal REAPDOR curve for spin-1 nuclei and to define the conditions for its application. We believe that we have satisfactorily achieved this by the numerical analysis. Nevertheless, it remains instructive to review the spin dynamics of the processes underlying the recoupling mechanism. We begin with

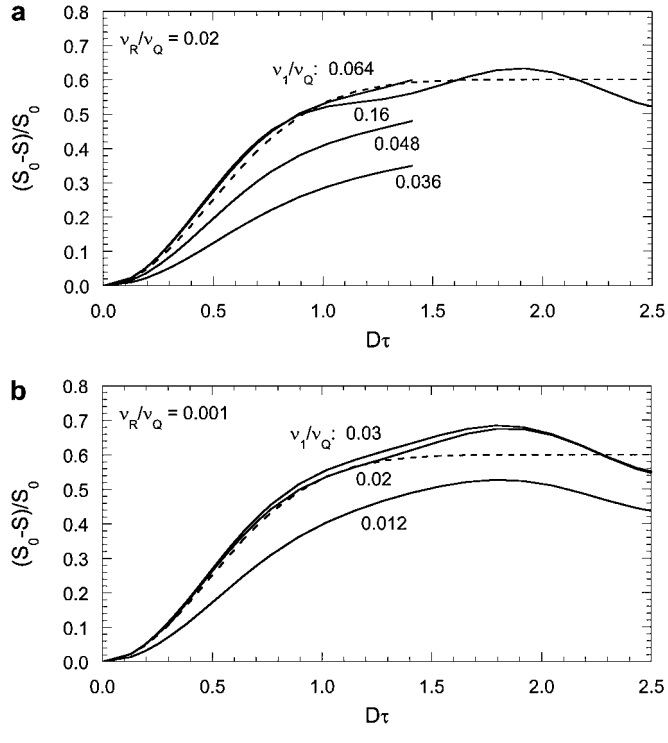

FIG. 4. REAPDOR dephasing curves for recoupling of spin-1 nuclei calculated with the indicated ratios of the rotation speed ν_R, the recoupling pulse amplitude ν_1, and the quadrupole frequency ν_Q. Actual parameters used in the calculations and resulting D_{fit}/D from curve fitting: (a) $\nu_Q = 250$ kHz, $\nu_R = 5$ kHz, $D = 160$ Hz, $\nu_1 = 9$, 12, 16, 40 kHz, $D_{\text{fit}}/D = 0.54$, 0.76, 1.05, 1.05, respectively; (b) $\nu_Q = 5000$ kHz, $\nu_R = 5$ kHz, $D = 160$ Hz, $\nu_1 = 60$, 100, and 150 kHz, $D_{\text{fit}}/D = 0.70$, 1.03, 1.06, respectively. For all curves, $\eta = 0$, $\theta = 90°$.

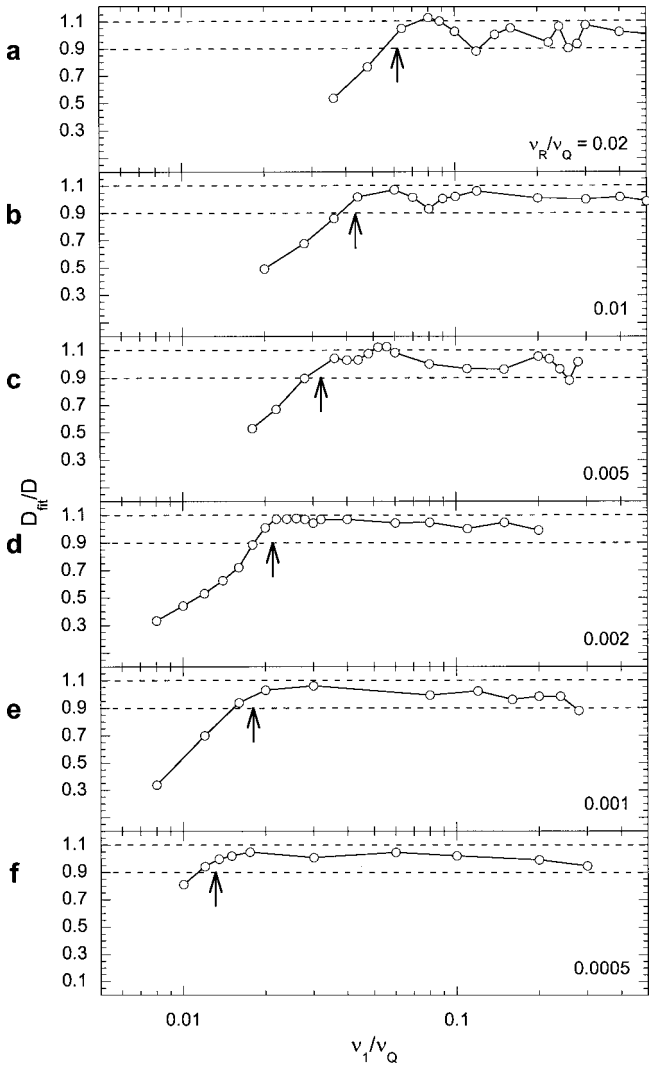

FIG. 5. Apparent dipolar coupling constants D_{fit} obtained by curve fitting of the universal dephasing curve to numerically calculated REAPDOR curves. The curves were calculated using the parameters listed in Table 2. For all curves, $\eta = 0$, $\theta = 90°$. The six plots are for the six indicated ν_R/ν_Q ratios. The fitted dipolar coupling constants are plotted as ratios D_{fit}/D where D is the value used in the actual calculations.

recalling that in a product-operator formalism of an observed spin I evolving under a dipolar interaction with a nonobserved spin S, the S portion of the expressions involves only the operators S_z, S_zI_x, and S_zI_y (*40*). Other coherences of S are not responsible for dipolar dephasing of I. This implies that we can restrict the physical description of the state of the $S = 1$ spins to a discussion of the populations of their spin states $m = 1$, 0, -1. Of course, other coherences of S play a crucial role in the inversion process during the recoupling pulse. However, we can assume here for simplicity that the duration τ_p of the inversion pulse is much shorter than the total duration τ of the dipolar evolution; consequently, the partial inversion of the quadrupolar S spins by the adiabatic-passage pulse can be considered as a sudden event. When the S-channel pulse is absent, the train of π pulses in the second half of the pulse sequence refocuses the dipolar dephasing that was introduced by the π pulses during the first half of the sequence. The refocusing is complete in this case, because the local field generated by the S spin at the site of the I spin is the same in the first and second halves of the sequence. On the other hand, when the S-channel recoupling pulse is present, the resulting change in the populations of the m-states of the S-spins causes the local fields at the I-spins to be different during the second half of the sequence and prevents complete refocusing.

The objectives of most heteronuclear recoupling strategies can be understood as manipulations of the populations of the m states. For instance, in a version of REDOR similar to our REAPDOR experiment (*47*), the desired change is achieved by a single π pulse on the S-channel, which inverts the populations ($m = 1 \leftrightarrow m = -1$; $m = 0$ unaffected). In θ-REDOR (*48*) the same transformations are made, but only partially. In DEAR and RIDER (*37, 38*), no RF pulse is applied but transitions among m states occur spontaneously as a result of spin–lattice relaxation. In those experiments, the change of the m-populations is a gradual process throughout the τ period rather than a one-time event at the center. The intent of TRAPDOR and REAPDOR is to induce adiabatic transfers of populations among the m states. Such transfers occur whenever the function $g_Q(t)$ describing the time dependence of the quadrupolar splitting (Eq. [7]) passes through zero in the presence of a strong RF amplitude, ν_1. The adiabatic population transfers are

$$m = 1 \rightarrow m = 0; \qquad m = 0 \rightarrow m = -1; \qquad m = -1 \rightarrow m = 1 \qquad [13]$$

or vice versa, depending on the sign of the slope of $g_Q(t)$ around $g_Q(t) = 0$.

The variability of the REAPDOR curves reviewed in the preceding paragraphs is exclusively caused by differences in the detailed behavior of the adiabatic passages. The timing and the degree of efficiency of the S-spin transitions are two sources for this variability to be considered. The time at which a specific crystallite will undergo an adiabatic transfer among its m-state populations coincides with a zero-crossing of $g_Q(t)$. REAPDOR

TABLE 2
Parameters Used for the Numerical REAPDOR Calculation Results Shown in Fig. 5 and Table 1

Figure	ν_R/ν_Q	ν_Q (kHz)	ν_R (kHz)	ν_1 (kHz)	D (Hz)
na	0.05	250	12.5	12–60	400
5a	0.02	250	5	18–65	160
5b	0.01	500	5	10–100	160
5c	0.005	2500	12.5	45–130	400
5d	0.002	2500	5	25–80	160
5e	0.001	5000	5	40–1200	160
5f	0.0005	10,000	5	100–175	160

dephasing due to adiabatic passages takes place only for those crystallites that have an odd number of crossings during the pulse. For the other crystallites, which have zero or an even number of zero-crossings, the spins are transferred back the original m-states and emerge from the pulse with no net change in their spin populations. Thus the REAPDOR dephasing depends on the fraction of the crystallites that undergo an odd number of zero-crossings during the pulse (*39*). The contribution of a particular crystallite to the signal decay is further determined by its integrated dipolar dephasing before and after the passages and, hence, depends on the points in time during the cycle of the function $g_D(t)$ at which the transfers occur. Thus the relative time dependences of $g_D(t)$ and $g_Q(t)$ determine the amount of dephasing. This explains the variability of the REAPDOR curve with changing η, θ, and ϕ. The numerical results showed that this effect is rather limited. This is due to the relatively short duration of the recoupling pulse in the REAPDOR pulse sequence. It is one of the advantages of REAPDOR over its predecessor TRAPDOR, where the recoupling pulse may stretch over an entire half of the τ period, thus enhancing the dependence on η, θ, and ϕ (*32, 39*).

As to the efficiency of the passages, we note that the REAPDOR dephasing is largest when the population transfers among the m-states are optimized. This is achieved when the passages are truly adiabatic, that is, when the passages are slow and in the presence of strong RF irradiation. The exact condition for adiabaticity varies for the different crystallites in a powder. Therefore, we adopt the previously proposed semi-quantitative test for the adiabaticities of level crossings of all crystallite orientations in a powder which states that the parameter $\alpha = \nu_1^2/\nu_Q\nu_R$ must be of an order of magnitude of at least 1 (*32, 33*). The numerical results reviewed above corroborate the validity of this concept. The broken line in Fig. 2b is a graphical representation of the condition $\alpha = 0.25$. It shows that in order to achieve universal REAPDOR behavior the passages of the quadrupole energy levels during the recoupling pulse must be adiabatic in nature and that the quantitative condition for adiabaticity is approximately given by $\alpha > 0.25$ for the case of spin-1 nuclei.

The notion of population transfers among well-defined spin states in the presence of RF irradiation loses its meaning when the RF amplitude, ν_1, is not much smaller than the quadrupole frequency, ν_Q. The irradiation then ceases to be selective to individual spin transitions. This has a profound effect on the way the recoupling pulse produces transfers among m-state populations, as is illustrated by an example shown in Fig. 6. The figure shows results of numerical calculations for a spin-1, which has an initial population of only its state $m = 1$ and which is then subjected to an RF pulse of duration $\tau_R/3$ under magic-angle spinning. The asymmetry parameter of the quadrupole tensor and its orientation in the rotor frame were chosen such that the number of zero crossings of $g_Q(t)$ during the pulse was either zero or one, depending on the phase of the sample rotation at the beginning of the pulse. Figure 6 plots the resulting populations

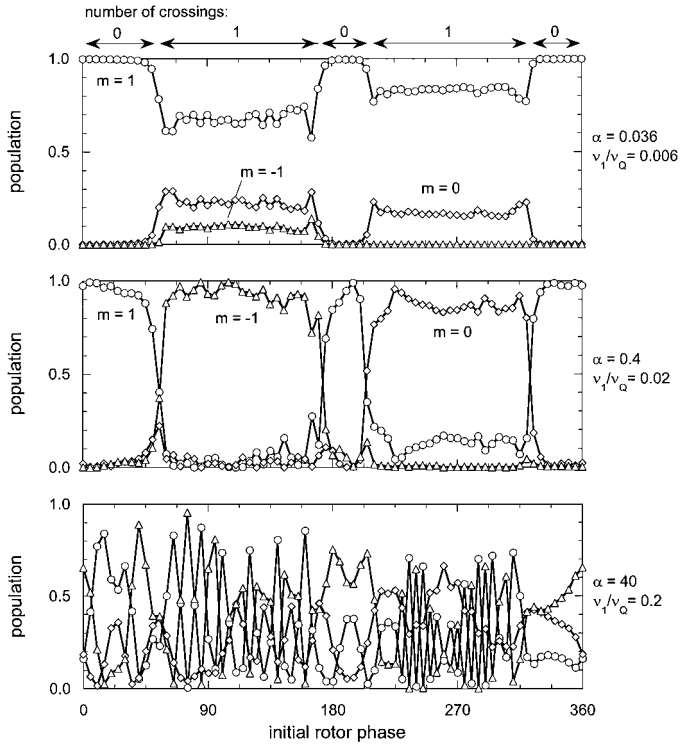

FIG. 6. Calculated populations of the three m-states of a spin-1 following the application of an RF pulse of duration $\tau_R/3$ under magic-angle spinning. Before the pulse the populations of the states $m = 1$, 0, and -1 were 1, 0, and 0, respectively. The calculations were performed for a single spin with a fixed position in the rotor frame and with 72 different initial phases of the sample rotation. The number of zero crossings of $g_Q(t)$ during the length of the pulse is either 0 or 1, depending on the initial rotor phase as indicated above the figure. Besides the adiabaticity parameters and the ν_R/ν_Q ratios indicated next to the plots, these numerical experiments are defined by the following quantities: $\nu_R/\nu_Q = 0.001$, $\nu_0/\nu_Q = 1000$, $\Delta\nu/\nu_Q = 0.1$, $\eta = 0.5$, $\chi = 45°$, $\psi = 45°$, where ν_0 is the Larmor frequency (determining the size of the second-order quadrupole term); $\Delta\nu$ is the frequency offset of the RF with respect to ν_0; χ and ψ are the polar angles of the rotor axis direction with respect to the quadrupole tensor; and the other parameters are as defined in the text.

of the three m-states as a function of the initial rotation phase. Further details are provided in the figure caption. The three examples given in Fig. 6 are for a nonadiabatic ($\alpha = 0.036$) and an adiabatic case ($\alpha = 0.4$) of selective irradiation ($\nu_1/\nu_Q \leq 0.02$) and for a case with a nonselective RF amplitude ($\nu_1/\nu_Q = 0.2$). For the $\alpha = 0.036$ and $\alpha = 0.4$ cases, hardly any change occurs when the number of crossings is 0 and there is an orderly transfer of populations between states when the number of crossings is 1, with the transfer being essentially complete for $\alpha = 0.4$. By contrast, the population transfers in the case of nonselective irradiation are unrelated to the number of level crossings and, in fact, appear to be random in nature. Despite this major difference between the effects of selective and nonselective pulses, the resulting REAPDOR curves are indistinguishable, as is apparent from the flat D_{fit}/D plots in Fig. 5. This suggests that the *average* Δm jump remains comparable in size over a wide range of RF amplitudes. After integration over a powder, it does

not make a difference if the changes in the m-state populations of the S spins were produced in an orderly or a random fashion. In any case, for a hypothetical model where the population transfer due to the recoupling pulse is assumed to be totally random, the REAPDOR curve can readily be predicted as follows. The REAPDOR curve for the subset of spins $S = 1$ that jump from m to $m \pm 1$ is identical to the well-known REDOR curve for the spin pair $I = 1/2$, $S = 1/2$ (*18–20*). Let us introduce the notation $R_{1/2}(D\tau)$ for the standard REDOR function. The REAPDOR curve for the spins that jump from m to $m \pm 2$ is then $R_{1/2}(2D\tau)$ and for those that do not change their m state it is 0. An enumeration of the nine $m \rightarrow m'$ possibilities in a random transfer model leads to the measured REAPDOR curve given by

$$(S_0 - S)/S_0 = (4/9)R_{1/2}(D\tau) + (2/9)R_{1/2}(2D\tau). \qquad [14]$$

Figure 7 compares this function with the universal REAPDOR curve described by Eq. [1]. There is no dependence on η, θ, and ϕ in this model since the transfers are not correlated with the function $g_Q(t)$. For $D\tau < 1$, Eq. [14] nearly coincides with the universal curve. Curve fitting gives $D_{\text{fit}}/D = 1.09$. Also, this particular linear combination of $R_{1/2}(D\tau)$ and $R_{1/2}(2D\tau)$ gives rise to the maximum around $D\tau = 1.8$. The fact that this feature is seen in all the numerical REAPDOR curves indicates that the adiabatic transfers affected by a pulse of duration $\tau_R/3$ mix the level populations to the same extent as random scrambling. In this context it is of interest to note that the universal curve proposed by Gullion (*34*) and by Ba *et al.* (*39*) for the description of the adiabatic case is, in fact, based on assumptions similar to those of the random-transfer model. In their model, the dephasing curve is derived from an enumeration of the fraction ξ of crystallites in a powder whose spins undergo an odd number of zero-crossings during the pulse. Orientational effects related to η, θ, and ϕ are assumed to be negligible. The result is a function that is equal to Eq. [14] multiplied by a factor $3\xi/2$. Their calculations showed that for a pulse duration of $\tau_R/3$ the fraction ξ is 0.667 which is, incidentally, the value required for exact numerical agreement between their simplified adiabatic model and our random-transfer model. This is probably the reason why the results of the present quantum mechanical calculations for $\tau_p = \tau_R/3$ showed no change in the REAPDOR curves when the RF amplitude increased from selective to nonselective irradiation. Nevertheless, we feel that Eq. [14] cannot serve as a quantitative standard for data analysis in a straightforward manner because the average value at long τ durations is high in comparison with that of the curves obtained in the more exact calculations.

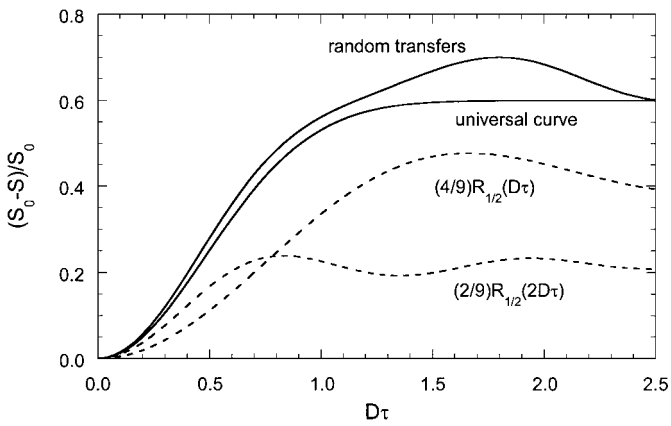

FIG. 7. Full lines, REAPDOR curve for a hypothetical model of random scrambling of the $S = 1$ level populations by the recoupling pulse, Eq. [14], compared with the universal REAPDOR curve, Eq. [1]. Broken lines, plots of the two contributions in Eq. [14] to the random-model curve. They are amplitude-reduced standard REDOR curves for $S = 1/2$ at regular and double time scales. Their sum reproduces the ubiquitous maximum of numerically calculated REAPDOR curves around $D\tau = 1.8$.

EXPERIMENTAL

The ^{14}N experiments were performed on a sample of alanine prepared by recrystallizing 10.0 mg [3-^{13}C; 99 at.%]L-alanine with 203.0 mg [^{15}N; 99 at.%]L-alanine. The labeled alanines were purchased from Cambridge Isotopes, Inc. The QCC of ^{14}N in alanine is 1.20 MHz (*50*), which corresponds to $\nu_Q = 1.81$ MHz (see Eq. [6]). The ^{2}D experiments were performed on a sample of alanine prepared by recrystallizing 20.6 mg [3-^{13}C, 2-^{2}D; 99 at.% and 98 at.%, respectively]DL-alanine with 408.8 mg DL-alanine. The labeled alanine was purchased from Isotec, Inc., and the natural-abundance alanine was purchased from Aldrich. The deuterium QCC for the labeled ^{2}D in this alanine sample is 167 kHz, which corresponds to $\nu_Q =$ 250 kHz.

Figure 1 shows the ^{13}C-observe REAPDOR experiment. Instead of the initial $\pi/2$ pulse shown in the figure, cross polarization from protons was used to generate the initial ^{13}C transverse magnetization and proton decoupling by a strong RF field was applied afterward. The train of π pulses on the ^{13}C channel during the dipolar evolution period was applied with the xy-4 phase cycle (*49*). The length of the S-spin recoupling pulse was $\tau_R/3$.

The magic-angle spinning NMR experiments were performed on a homebuilt triple-channel spectrometer operating at a proton frequency of 151.394 MHz. The spectrometer uses a Tecmag Libra pulse programmer. The triple-tuned MAS probe uses a Chemagnetics 7.5 mm spinning assembly and is of a transmission-line design. Proton radiofrequency (RF) field strengths were 50 kHz for cross-polarization and 110 kHz for proton decoupling. All cross-polarization contact times were 1 ms. The ^{13}C, RF field strength was 50 kHz. The ^{14}N RF field strengths ν_1 were varied from 13.5 to 54.1 kHz, and the ^{2}D RF field strengths were varied from 7.5 to 53.6 kHz. The sample spinning rate was set to either 800, 2000, 3125, or 3861 Hz. The sample spinning rate stability is important for obtaining

good signal/noise ratios with the REAPDOR pulse sequence that we use here. Accordingly, the spinning rates were controlled to within 0.2 Hz of the desired values for the REAPDOR experiments using the method described below.

As mentioned above, it is best to control the sample spinning speed to the desired value as closely as possible. An examination of the ^{13}C part of the pulse sequence shows that the chemical shift anisotropy is not refocused until the end of the dipolar evolution period. Hence, if the ^{13}C π pulse train is not truly synchronous with the sample rotation, then incomplete refocusing of the ^{13}C magnetization occurs (*47, 51*). We present in this section some results obtained on a sample of natural-abundance alanine (Aldrich) with a spinning rate of 2000.0 Hz controlled to within 0.1 Hz. These results are presented to reinforce the need to have a system that has a stable spinning rate.

A CompAir Hydrovane rotary vane compressor provided compressed air for sample spinning. The compressor maintains a pressure between 90 and 110 psi in an attached 100-gallon ballast tank. This air is delivered to a 60-gallon tank regulated at 80 psi. The gas is then delivered to another 60-gallon tank with the gas pressure regulated at 60 psi. Two 30-gallon tanks feed off the latter tank; one of these is the source for the bearing air and is regulated at 40 psi and the other is the source for the drive air and is regulated at 25 psi. The function of all of these ballast tanks is to smooth any pressure waves that might be generated by the compressor.

Our spinning control system has been described in detail elsewhere, but we give a brief description of the system here (*51*). The sample rotor is marked with black ink to provide an alternating pattern of dark and light marks. Typically, we paint 5 marks on the rotor. The spinning speed is monitored optically by counting the number of times the black marks appear in one second. This number is compared to the expected number of passing black marks for the desired spinning rate. If the optically detected number of passing marks differs from the set value, then an electronically controlled air valve adjusts the drive gas pressure accordingly to compensate for the error in the spinning rate. With 5 marks painted on the rotor and a counting time of 1 s, the spinning rate can be corrected when the spinning rate deviates by 0.2 Hz from the set value.

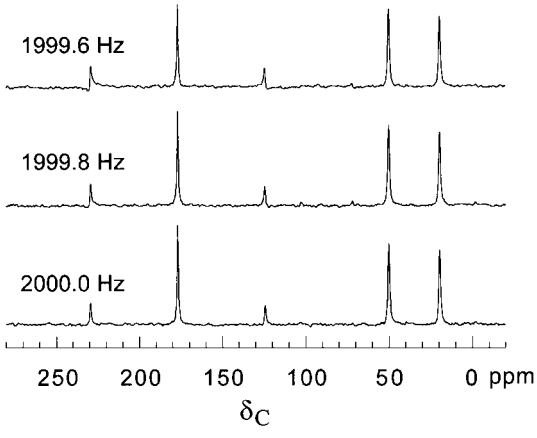

FIG. 8. ^{13}C spectra of natural abundance alanine taken with the pulse sequence of Fig. 1 with $N_c = 30$ and with the pulse timings set for an exact 2-kHz spinning rate.

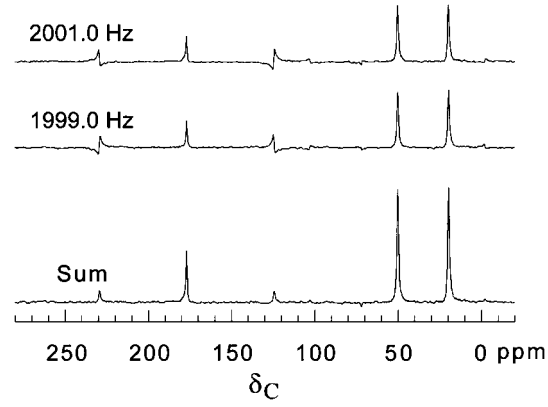

FIG. 9. ^{13}C spectra of natural abundance alanine obtained with the same conditions described in Fig. 8, but with the spinning speed deviations of $+1$ Hz and -1 Hz from the ideal. The sum of the $+$ and $-$ rate deviations leads to a properly phased spectrum that suffers significant signal attenuation.

Experiments to illustrate the effect of spinning rate stability were performed using the ^{13}C part of the REAPDOR pulse sequence with the pulse timings set for an expected spinning rate of 2000 Hz and the evolution period set to 30 rotor cycles. Ten marks were painted on the rotor and the marks counted for one second; the spinning rate was found to be stable to within 0.1 Hz for this setup. Figure 8 shows spectra taken with the spinning rate set to 2000.0, 1999.8, and 1999.6 Hz. As the spinning rate moves from the ideal 2000.0 Hz, distortions in the spinning sidebands of the carboxyl carbon appear and there is observable loss in intensity of the carboxyl carbon ^{13}C resonance. In ordinary experiments, the spinning rate will fluctuate above and below the desired spinning rate. The consequence of these fluctuations is that the spinning sidebands will appear normally phased. This effect is shown in Fig. 9 where spectra were taken at 2001.0 and 1999.0 Hz to illustrate what happens when fluctuations occur above and below the desired spinning rate. Both spectra show severe distortions in their sidebands, but in opposite directions. Also, both spectra show that a control of only 1 Hz in the spinning rate will result in significant signal loss, especially at the carboxyl carbon position. The sum of the two spectra results in normally phased spinning sidebands. Hence, poor spinning speed control may provide spectra with the appearance of good quality, but the signal-to-noise ratio will suffer considerably under these conditions.

RESULTS

REAPDOR curves for the methyl carbon were measured for ^{2}D–^{13}C and ^{14}N–^{13}C spin pairs in the samples described in the experimental section. The curves were fitted to the universal

dephasing curve and the resulting D_{fit} values were compared with the actual dipolar coefficient D calculated from the internuclear distances known from the crystal structure. The C–D distance is 2.17 Å and the C–N distance is 2.47 Å (*52*). These distances correspond to dipolar couplings of 450 and 144 Hz, respectively. The ^{14}N experiments were repeated for three spinning frequencies and a range of recoupling pulse amplitudes of the adiabatic pulse. The QCCs of the ^{2}D and ^{14}N nuclei mentioned under Experimental allow the corresponding ν_1/ν_Q and ν_R/ν_Q ratios to be evaluated. Figure 10 shows the resulting D_{fit}/D ratios plotted against ν_1/ν_Q. The arrows in the figure indicate the lower limits of the usable ν_1/ν_Q ranges. They were found by interpolation of the data points in Table 1 and Fig. 2b.

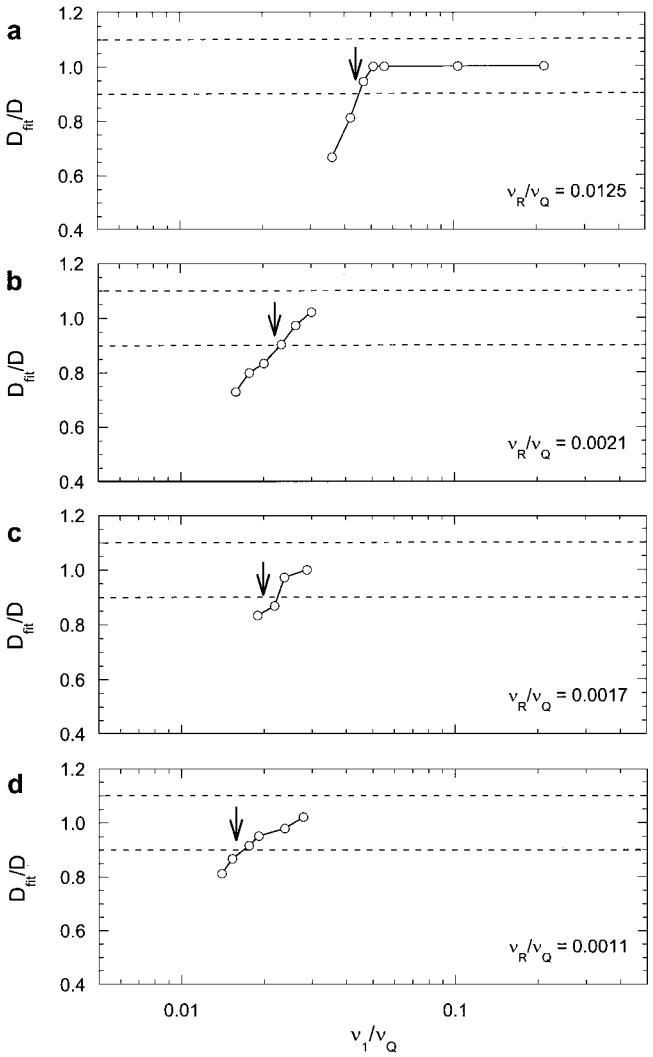

FIG. 10. Dipolar coupling constants obtained for alanine by curve fitting of the universal dephasing curve to measured REAPDOR curves. The fitted dipolar coupling constants D_{fit} are normalized to the D values derived from the crystal structure. The experimental parameters are listed in Table 3. The arrows indicate the lower boundaries of the useful region (interpolated from Fig. 2b and Table 1).

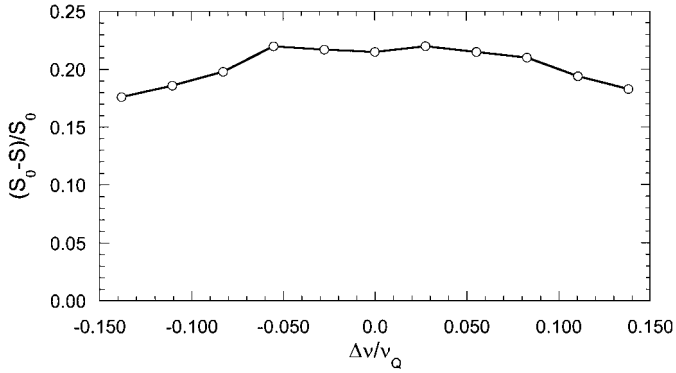

FIG. 11. REAPDOR fraction, $(S_0 - S)/S_0$, obtained for the methyl ^{13}C resonance of alanine as a function of the difference $\Delta\nu$ between the recoupling-pulse frequency and the ^{14}N Larmor frequency. Experimental parameters: $\nu_R = 800$ Hz, $\nu_1 = 42$ kHz, $\tau = 2.5$ ms, corresponding to $\nu_R/\nu_Q = 0.00044$, $\nu_1/\nu_Q = 0.0232$, $D\tau = 0.36$. The offset, ranging from -250 to $+250$ kHz, is plotted as the ratio $\Delta\nu/\nu_Q$.

These results indicate that the proposed method for analysis of REAPDOR data indeed yields dipolar coupling constants with better than $\pm 13\%$ accuracy, provided ν_1 and ν_R meet the required conditions. Finally, results of REAPDOR fractions measured as a function of the frequency offset $\Delta\nu$ of the recoupling pulse with respect to the resonance frequency of the ^{14}N resonance frequency of alanine are plotted in Fig. 11. The data demonstrate that the dephasing is not appreciably affected by offsets that are less than 5% of ν_Q (± 100 kHz in the alanine case).

DISCUSSION

We have established the ranges of rotation speeds, ν_R, and RF amplitudes, ν_1, for which experimental REAPDOR results with ^{2}D or ^{14}N as the nonobserved spin can be readily analyzed by comparison with the universal dephasing curve given in Eq. [1]. The limiting values of the ranges are given as fractions of the quadrupole frequency, ν_Q, and are shown in Fig. 2b. Provided the QCC, and hence ν_Q, is approximately known, the experimental parameters required for successful application of the universal curve can be chosen according to these boundary rules. An important benefit of the proposed approach is that knowledge of the asymmetry parameter of the quadrupolar tensor or of its orientation in the molecular frame is not required. In a typical case of

TABLE 3
Experimental Parameters Used in the REAPDOR Experiments on Alanine, the Results of Which Are Shown in Fig. 10

Figure	ν_R/ν_Q	ν_Q (kHz)	ν_R (kHz)	ν_1 (kHz)	D (Hz)
10a	0.0125	250	3.125	9.0–53.5	450
10b	0.00214	1800	3.861	28.7–54.1	144
10c	0.00174	1800	3.125	34.2–51.8	144
10d	0.00111	1800	2.000	25.2–50.0	144

^{14}N, the QCC is somewhat larger than in alanine, which was the example used in this paper. Thus, the conditions on the RF amplitude are more stringent in general applications, particularly if one works with a sample of which the QCC is not known. In most cases, the QCC of ^{14}N is 3.3 MHz or smaller, corresponding to $\nu_Q \leq 5$ MHz. (Typical QCCs are 2.4 MHz for amides, 1.2 and 2.5 MHz for amino acids, 3.3 MHz for peptide bonds, and 0.8 MHz for purines (*53*). This implies that when the QCC is unknown, the RF amplitude has to be at least 76 kHz with a spinning speed of 6 kHz, or 60 kHz with a spinning speed of 3 kHz. In the typical case of deuterium, having QCC $\sim$ 160 kHz ($\nu_Q \sim 240$ kHz), the RF amplitude has to be at least 22 kHz at a spinning speed of 10 kHz, or 17 kHz at a spinning speed of 5 kHz. Another useful feature of the REAPDOR experiment is that there is considerable leeway in the value of the applied *S*-spin RF frequency. Figure 11 shows that the *S*-spin irradiation frequency may deviate from the isotropic position by as much as 5% of the quadrupolar coupling frequency. This is particularly important in the case of ^{14}N, for which the isotropic shift is usually difficult to measure directly.

ACKNOWLEDGMENTS

This research project was supported by the US–Israel Binational Science Foundation and by NSF Grant CHE-0091663.

REFERENCES

1. D. P. Raleigh, M. H. Levitt, and R. G. Griffin, Rotational resonance in solid state NMR, *Chem. Phys. Lett*. **146,** 71–76 (1988).
2. D. P. Raleigh, A. C. Kolbert, T. G. Oas, M. H. Levitt, and R. G. Griffin, Enhancement of the effect of small anisotropies in magic-angle spinning nuclear magnetic resonance, *J. Chem. Soc. Faraday Trans. 1* **84,** 3691–3711 (1988).
3. M. H. Levitt, D. P. Raleigh, F. Creuzet, and R. G. Griffin, Theory and simulations of homonuclear spin pair systems in rotating solids, *J. Chem. Phys.* **92,** 6347–6364 (1990).
4. Y. K. Lee, N. D. Kurur, M. Helmle, O. G. Hohannessen, N. C. Nielsen, and M. H. Levitt, Efficient dipolar recoupling in the NMR of rotating solids: A sevenfold symmetric radiofrequency pulse sequence, *Chem. Phys. Lett*. **242,** 304–309 (1995).
5. J. H. Ok, R. G. S. Spencer, A. E. Bennett, and R. G. Griffin, Homonuclear correlation spectroscopy in rotating solids, *Chem. Phys. Lett.* **197,** 389–395 (1992).
6. R. Tycko and G. Dabbagh, Measurement of nuclear magnetic dipole-dipole couplings in magic angle spinning NMR, *Chem. Phys. Lett.* **173,** 461–465 (1990).
7. R. Tycko and S. O. Smith, Symmetry principles in the design of pulse sequences for structural measurements in magic angle spinning nuclear magnetic resonance, *J. Chem. Phys*. **98,** 932–943 (1993).
8. C. A. Klug, W. Zhu, M. E. Merritt, and J. Schaefer, Compensated XY8-DRAMA pulse sequence for homonuclear dephasing, *J. Magn. Reson*. **109,** 134–136 (1994).
9. D. M. Gregory, G. Wolfe, T. Jarvie, J. Shiels, and G. P. Drobny, Double-quantum filtering in magic angle spinning NMR spectroscopy applied to DNA oligomers, *Mol. Phys*. **89,** 1835–1849 (1996).
10. A. E. Bennett, J. H. Ok, R. G. Griffin, and S. Vega, Chemical shift correlation spectroscopy in rotating solids: Radiofrequency-driven dipolar recoupling and longitudinal exchange, *J. Chem. Phys*. **96,** 8624–8627 (1992).
11. T. Gullion and S. Vega, A simple magic angle spinning NMR experiment for the dephasing of rotational echoes of dipolar coupled homonuclear spin pairs, *Chem. Phys. Lett*. **194,** 423–428 (1992).
12. B. Q. Sun, P. R. Costa, D. Kocisko, P. T. Lansbury, and R. G. Griffin, Internuclear distance measurements in solid state nuclear magnetic resonance: Dipolar recoupling via rotor synchronized spin locking, *J. Chem. Phys*. **102,** 702–707 (1995).
13. C. M. Rienstra, M. E. Hatcher, L. J. Mueller, B. Sun, S. W. Fesik, and R. G. Griffin, Efficient multispin homonuclear double-quantum recoupling for magic-angle spinning NMR: 13C-13C correlation spectroscopy of U-13C-erythromycin A, *J. Am. Chem. Soc*. **120,** 10602–10612 (1998).
14. M. Hohwy, H. J. Jakobsen, M. Eden, M. H. Levitt, and N. C. Nielsen, Broadband dipolar recoupling in the nuclear magnetic resonance of rotating solids: A compensated C7 pulse sequence, *J. Chem. Phys.* **108,** 2686–2694 (1998).
15. M. Howry, C. M. Rienstra, C. P. Jaroniec, and R. G. Griffin, Fivefold symmetric homonuclear dipolar recoupling in rotating solids: Application to double quantum spectroscopy, *J. Chem. Phys.* **110,** 7983–7992 (1999).
16. A. Brinkmann, M. Eden, and M. H. Levitt, Synchronous helical pulse sequences in magic-angle spinning nuclear magnetic resonance: Double quantum recoupling of multiple-spin systems, *J. Chem. Phys.* **112,** 8539–8554 (2000).
17. I. Yoshitaka, 13C-13C Dipolar recoupling under very fast magic angle spinning in solid-state nuclear magnetic resonance: Applications to distance measurements, spectral assignments, and high-throughput secondary-structure determination, *J. Chem. Phys.* **114,** 8473–8483 (2001).
18. T. Gullion and J. Schaefer, Rotational-echo double-resonance NMR, *J. Magn. Reson*. **81,** 196–200 (1989).
19. T. Gullion and J. Schaefer, Detection of weak heteronuclear dipolar couplings by rotatonal-echo, double-resonance nuclear magnetic resonance, *in* "Advances in Magnetic Resonance" (W. S. Warren, Ed.), Vol. 13, pp. 57–83, Academic Press, New York, 1989.
20. T. Gullion, Measurement of heteronuclear dipolar interactions by rotational-echo, double-resonance nuclear magnetic resonance, *Magn. Reson. Rev*. **17,** 83–131 (1997).
21. A. W. Hing, S. Vega, and J. Schaefer, Transfer-echo, double-resonance NMR, *J. Magn. Reson*. **96,** 205–209 (1992).
22. T. G. Oas, R. G. Griffin, and M. H. Levitt, Rotary resonance recoupling of dipolar interactions in solid-state magnetic resonance spectroscopy, *J. Chem. Phys*. **89,** 692–695 (1988).
23. C. Fernandez, D. P. Lang, J. P. Amoureux, and M. Pruski, Measurement of heteronuclear dipolar interactions between quadrupolar and spin-1/2 nuclei in solids by multiple-quantum REDOR NMR, *J. Am. Chem. Soc*. **120,** 2672–2673 (1998).
24. A. Schmidt, R. A. Mackay, and J. Schaefer, Internuclear distance measurement between deuterium (I = 1) and a spin-1/2 nucleus in rotating solids, *J. Magn. Reson*. **96,** 644–650 (1992).
25. D. Sandstrom, M. Hong, and K. Schmidt-Rohr, Identification and mobility of deuterated residues in peptides and proteins by solid-state NMR, *Chem. Phys. Lett*. **300,** 213–220 (1999).
26. I. Sack, A. Goldburt, S. Vega, and G. Buntkowsky, Deuterium REDOR: Principles and applications for distance measurements, *J. Magn. Reson*. **138,** 54–65 (1999).
27. I. Sack, Y. S. Balazs, S. Rahimipour, and S. Vega, Solid-state NMR determination of peptide torsion angles: Applications of ^{2}H-dephased REDOR, *J. Am. Chem. Soc*. **122,** 12263–12269 (2000).
28. T. Gullion, A comparison between REDOR and θ-REDOR for measuring 13C-2D dipolar interactions in solids, *J. Magn. Reson*. **139,** 402–407 (1999).

29. T. Gullion, Measuring 13C-2D dipolar couplings with a universal REDOR dephasing curve, *J. Magn. Reson*. **146,** 220–222 (2000).
30. E. R. H. van Eck, R. Janssen, W. E. J. R. Maas, and W. S. Veeman, A novel application of nuclear spin-echo, double-resonance to aluminophosphates and aluminosilicates, *Chem. Phys. Lett*. **174,** 428–432 (1990).
31. C. P. Grey, W. S. Veeman, and A. J. Vega, Rotational echo 14N/13C/1H triple resonance solid state nuclear magnetic resonance: A probe of 13C-14N internuclear distances, *J. Chem. Phys*. **98,** 7711–7724 (1993).
32. C. P. Grey and A. J. Vega, Determination of the quadrupolar coupling constant of the invisible aluminum spins in zeolite HY with 1H/27Al TRAPDOR NMR, *J. Am. Chem. Soc*. **117,** 8232–8242 (1995).
33. C. P. Grey, W. S. Veeman, and A. J. Vega, Rotational-echo, nitrogen-14/carbon-13/proton triple resonance, solid-state, nuclear magnetic resonance: A probe of carbon-13-nitrogen-14 internuclear distances, *J. Chem. Phys*. **98,** 7711–7724 (1993).
34. T. Gullion, Measurement of dipolar interactions between spin-1/2 and quadrupolar nuclei by rotational-echo, adiabatic-passage, double-resonance NMR, *Chem. Phys. Lett.* **246,** 325–330 (1995).
35. T. Gullion, Detecting 13C-17O dipolar interactions by rotational-echo, adiabatic-passage, double-resonance NMR, *J. Magn. Reson. A* **117,** 326–329 (1995).
36. L. Chopin, S. Vega, and T. Gullion, A MAS NMR method for measuring ^{13}C-^{17}O distances, *J. Am. Chem. Soc.* **120,** 4406–4409 (1998).
37. J. R. Sachleben, V. Frydman, and L. Frydman, Dipolar determination in solids by relaxation-assisted NMR recoupling, *J. Am. Chem. Soc*. **118,** 9786–9787 (1996).
38. K. Saalwachter and K. Schmidt-Rohr, Relaxation-induced dipolar exchange with recoupling—An MAS NMR method for determining heteronuclear distances without irradiating the second spin, *J. Magn. Reson*. **145,** 161–172 (2000).
39. Y. Ba, H. Kao, C. P. Grey, L. Chopin, and T. Gullion, Optimizing the 13C-14N REAPDOR NMR experiment: A theoretical and experimental study, *J. Magn. Reson*. **133,** 104–114 (1998).
40. R. R. Ernst, G. Bodenhausen, and A. Wokaun, "Principles of Nuclear Magnetic Resonance in One and Two Dimensions," Clarenden, Oxford, 1987.
41. D. Freude and J. Haase, *NMR Basic Principles Progr.* **29,** 1–90 (1993).
42. D. Freude, Quadrupolar nuclei in solid-state nuclear magnetic resonance, *in* "Encyclopedia of Analytical Chemistry" (R. A. Meyers, Ed.), p. 12188, Wiley, Chichester, 2000.
43. A. E. Bennet, R. G. Griffin, and S. Vega, *NMR Basic Principles Progr.* **33,** 1 (1994).
44. C. P. Slichter, "Principles of Magnetic Resonance," Springer-Verlag, New York, 1996.
45. H. Conroy, Molecular Schrodinger equation. VIII. A new method for the evaluation of multidimensional integrals, *J. Chem. Phys.* **47,** 5307–5318 (1967).
46. K. T. Mueller, T. P. Jarvie, D. J. Aurentz, and B. W. Roberts, The REDOR transform: Direct calculation of internuclear couplings from dipolar-dephasing NMR data, *Chem. Phys. Lett.* **242,** 535–542 (1995).
47. J. R. Garbow and T. Gullion, Improvements in REDOR NMR spectroscopy: Minimizing resonance-offset effects, *J. Magn. Reson*. **95,** 442–445 (1991).
48. T. Gullion and C. Pennington, θ-REDOR: An MAS NMR method to simplify multiple coupled heteronuclear spin systems, *Chem. Phys. Lett*. **290,** 88–93 (1998).
49. T. Gullion, D. B. Baker, and M. S. Conradi, New, compensated Carr–Purcell sequences, *J. Magn. Reson*. **89,** 479–484 (1990).
50. M. J. Hunt and A. L. Mackay, Deuterium and nitrogen pure quadrupole resonance in deuterated amino acids, *J. Magn. Reson*. **15,** 402–414 (1974).
51. L. Chopin, R. Rosanske, and T. Gullion, Simple improvements in spinning-speed control for MAS NMR experiments, *J. Magn. Reson. A* **122,** 237–239 (1996).
52. M. S. Lehmann, T. G. Koetzle, and W. C. Hamilton, Precision neutron diffraction structure determination of protein and nucleic acid components. I. The crystal and molecular structure of the amino acid L-alanine, *J. Am. Chem. Soc*. **94,** 2657–2660 (1972).
53. D. T. Edmonds, *Phys. Rep.* **29,** 233–290 (1977).